Electronic Supplementary Material (ESI) for Dalton Transactions.

Quaternary alkaline-earth metal thiophosphate $SrAgPS_4$: syntheses, structure, and optical properties

Wenhao Xing,[⊥[a]] Jian Tang,[⊥[a]] Liang Fei,[[b]] Chunlan Tang[[a,c]], Jieyun Wu[[c]],Wenlong Yin,*[[a]] Bin Kang[[a]] and Jianguo Deng[[a]]

a. Institute of Chemical Materials, China Academy of Engineering Physics, Mianyang 621900, People's Republic of China. E-mail: wlyin@caep.cn

b. Key Laboratory of Science and Technology on High Energy Laser, China Academy of Engineering Physics, Mianyang 621900, People's Republic of China.

c. Institute of Chemical Materials, China Academy of Engineering Physics, Mianyang 621900, P.R. China.

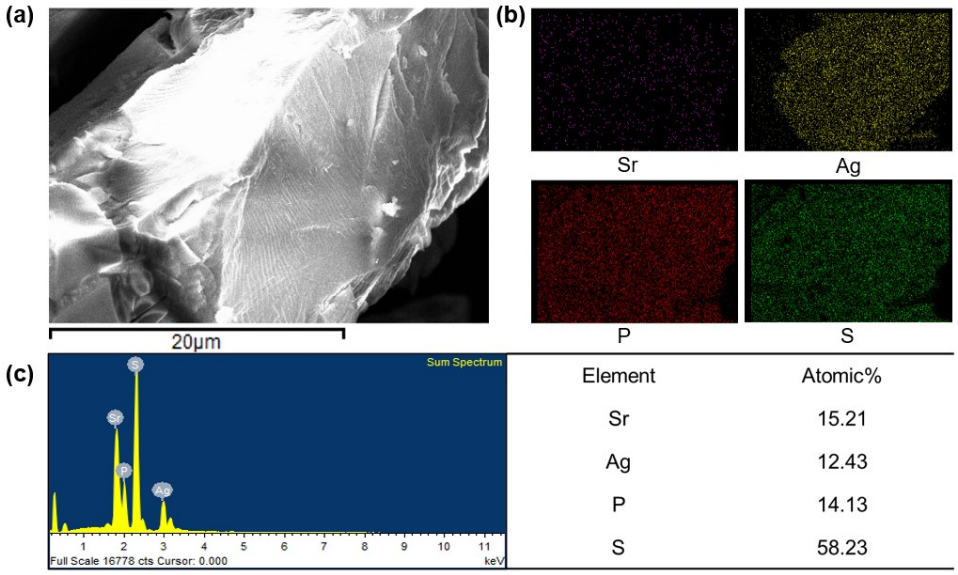

Figure S1 (a) Scanning electron microscopy (SEM) image of $SrAgPS_4$; (b) Elemental distribution of the as-grown crystal (from left to right: Sr, Ag, P, S). (c) Elemental analysis of $SrAgPS_4$ by EDX spectroscopy.

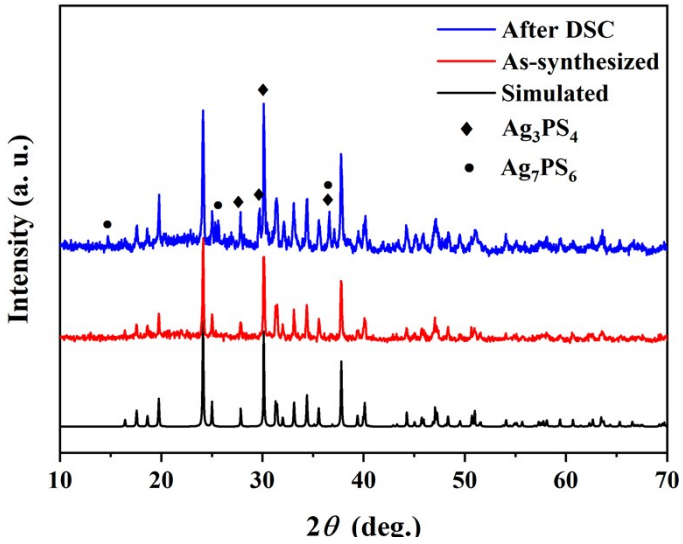

Figure S2 Powder XRD patterns of $SrAgPS_4$ before and after differential scanning calorimetry measurement.

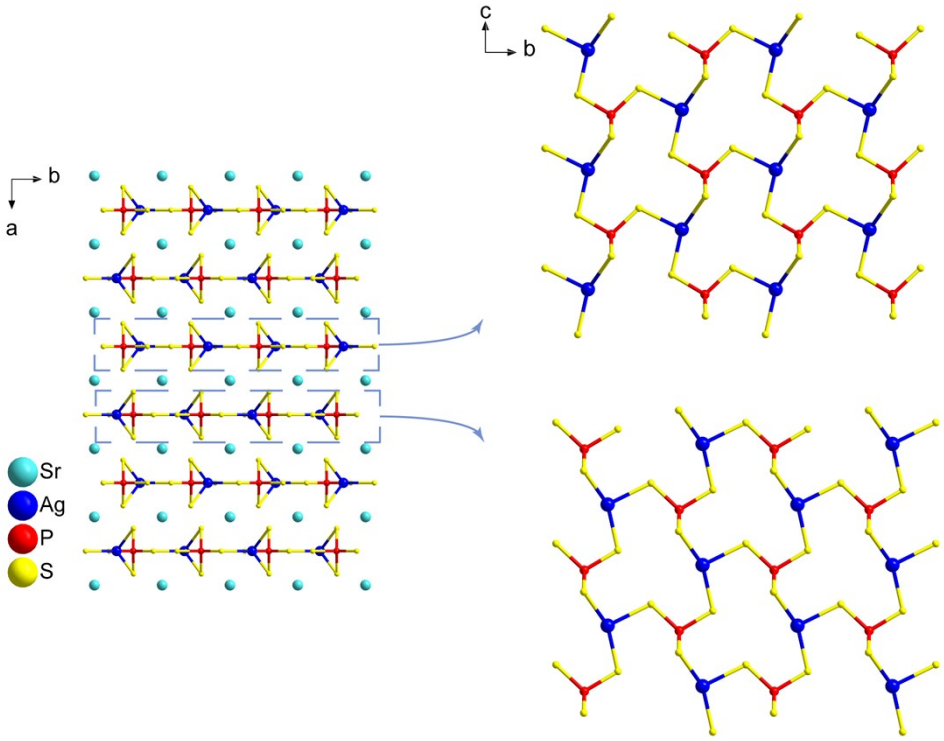

Figure S3 Two adjacent layers are arranged antiparallel to each other.

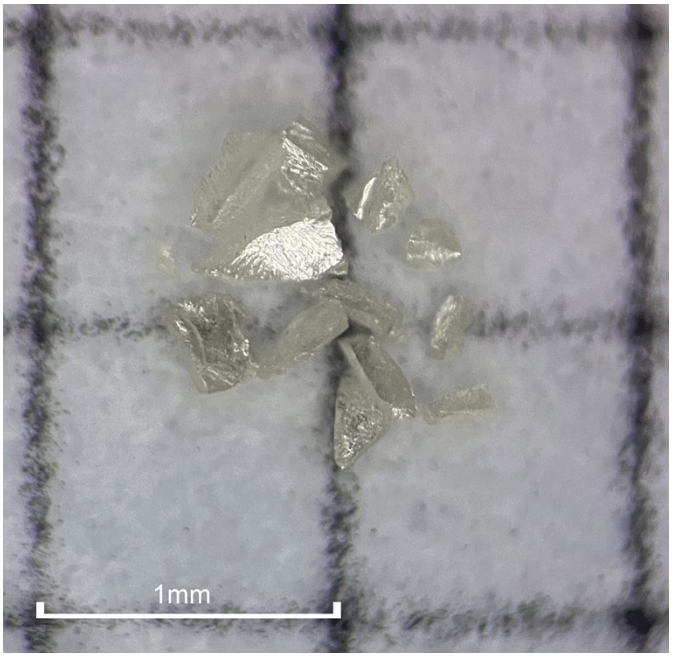

Figure S4 The Photo of SrAgPS4 crystals.

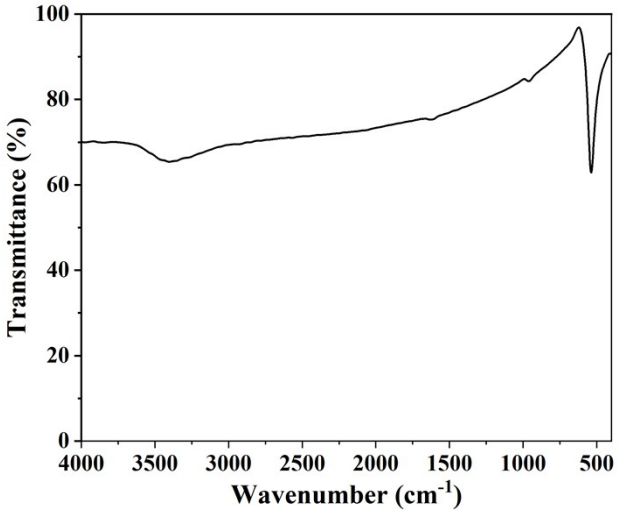

Figure S5 FT-IR spectra for SrAgPS4.

Table S1 Selected Bond Lengths (Å) and Bond Angles (°) for $SrAgPS_4$.

Sr1—S1	3.0053 (12)	Ag1A—S2^{vi}	2.761 (5)
Sr1—S1^{i}	3.0053 (12)	Ag1A—S3^{iv}	2.552 (7)
Sr1—S3^{ii}	3.0789 (15)	Ag1B—S1^{vii}	2.469 (5)
Sr1—S3^{iii}	3.0789 (15)	Ag1B—S2^{vi}	2.509 (5)
Sr1—S2^{i}	3.1731 (16)	Ag1B—S3^{iv}	2.622 (7)
Sr1—S2^{iv}	3.1740 (18)	P1—S1	2.062 (3)
Sr1—S2^{v}	3.1740 (18)	P1—S2	2.040 (2)
Sr1—S2	3.1731 (17)	P1—S2^{vii}	2.040 (2)
Ag1A—S1	2.473 (6)	P1—S3	2.049 (3)
S1—Ag1A—S3^{iv}	104.0 (3)	S1—Ag1B—S3^{iv}	102.1 (2)
S1—Ag1A—S2^{viii}	136.89 (15)	S1—Ag1B—S2^{vi}	156.1 (3)
S1—Ag1A—S2^{vi}	136.89 (15)	S2^{vi}—Ag1B—S3^{iv}	101.76 (18)
S3^{iv}—Ag1A—S2^{vi}	96.99 (18)	S3—P1—S1	106.05 (14)
S3^{iv}—Ag1A—S2^{viii}	96.99 (18)	S2^{vii}—P1—S1	107.32 (8)
S2^{vi}—Ag1A—S2^{viii}	75.22 (17)	S2—P1—S1	107.32 (8)
Sr1^{ix}—Ag1B—Sr1^{x}	101.5 (4)	S2—P1—S3	112.18 (9)
S1—Ag1B—Sr1^{x}	102.4 (3)	S2^{vii}—P1—S3	112.18 (9)
S1—Ag1B—Sr1^{ix}	140.9 (7)	S2—P1—S2^{vii}	111.41 (15)

Symmetry codes: (i) −*x*+1, −*y*+1, *z*; (ii) −*x*+1, −*y*+3/2, *z*−1/2; (iii) *x*, *y*−1/2, *z*−1/2; (iv) *x*, *y*−1/2, *z*+1/2; (v) −*x*+1, −*y*+3/2, *z*+1/2; (vi) −*x*+3/2, *y*, *z*+1; (vii) −*x*+3/2, *y*, *z*; (viii) *x*, *y*, *z*+1; (ix) *x*+1/2, −*y*+1, *z*+1; (x) *x*+1/2, −*y*+3/2, *z*+1/2.

Table S2 Fractional Atomic Coordinates ($\times 10^4$) and Equivalent Isotropic Displacement Parameters ($Å^2 \times 10^3$) for $SrAgPS_4$. U_{eq} is defined as 1/3 of the trace of the orthogonalised U_{IJ} tensor.

Atom	Wyckoff site	*Occupancy*	*x*	*y*	*z*	U(eq)
Sr^1	4a	1	5000	5000	2962.4(17)	16.6(3)
Ag^{1A}	4b	0.50(5)	7500	6626(7)	8624(9)	47(4)
Ag^{1B}	8c	0.25(3)	8170(30)	6560(9)	8489(13)	54(4)
P^1	4b	1	7500	7861.8(19)	3208(4)	8.7(5)
S^1	4b	1	7500	6093(2)	4851(4)	11.9(5)
S^2	8c	1	5830.8(18)	7886.3(16)	1413(3)	16.6(4)
S^3	4b	1	7500	9349(2)	5402(4)	15.4(5)

Table S3 Bond valence sums for $SrAgPS_4$.

Atom	Valence	BVSum
Sr1	2.000	2.011
Ag1A	1.000	1.044
Ag1B	1.000	1.083
P1	5.000	5.206
S1	-2.000	2.292
S2	-2.000	2.111
S3	-2.000	1.939

Table S4 Structure and properties comparison of $SrCdGeS_4$-type compounds crystallized in the orthorhombic system space group of *Ama*2.

Compounds	Space Group	E_g (eV)	SHG (×AGS)	Phase-matching	Congruent-melting (Tm/Tc)	Ref.
$SrCdGeS_4$	*Ama*2	2.6	1.7	yes	987/946	[1]
$EuCdGeS_4$	*Ama*2	2.5	2.6	yes	997/864	[2]
$EuCdGeSe_4$	*Ama*2	2.25	3.8	yes	882/723	[2]
$BaHgGeSe_4$	*Ama*2	2.49	4.7	yes	732/589	[3]
$SrHgGeSe_4$	*Ama*2	2.42	4.8	yes	745/684	[3]
β-$BaHgSnS_4$	*Ama*2	2.77	2.8	yes	no	[4]
$SrHgSnS_4$	*Ama*2	2.72	1.9	yes	no	[4]
$EuHgGeS_4$	*Ama*2	2.04	0.9	yes	-	[5]
$EuHgGeSe_4$	*Ama*2	1.97	3.1	yes	764/651	[6]
$EuHgSnS_4$	*Ama*2	2.14	1.77	yes	no	[6]
$SrAgAsS_4$	*Ama*2	2.31	1.35	yes	no	[7]
$SrAgPS_4$	*Ama*2	2.97	1.10	yes	no	This work

Reference

[1] Y. Dou, Y. Chen, Z. Li, A.K. Iyer, B. Kang, W. Yin, J. Yao, A. Mar, $SrCdGeS_4$ and $SrCdGeSe_4$: Promising Infrared Nonlinear Optical Materials with Congruent-Melting Behavior, Cryst. Growth Des. 19 (2019) 1206-1214.

[2] Y. Guo, F. Liang, W. Yin, Z. Li, X. Luo, Z.-S. Lin, J. Yao, A. Mar, Y. Wu, $BaHgGeSe_4$ and $SrHgGeSe_4$: Two New Hg-Based Infrared Nonlinear Optical Materials, Chem. Mater. 31 (2019) 3034-3040.

[3] W. Xing, N. Wang, Y. Guo, Z. Li, J. Tang, K. Kang, W. Yin, Z. Lin, J. Yao, B. Kang, Two rare-earth-based quaternary chalcogenides $EuCdGeQ_4$ (Q = S, Se) with strong second-harmonic generation, Dalton Trans. 48 (2019) 17620-17625.

[4] Y. Guo, F. Liang, Z. Li, W. Xing, Z.-s. Lin, J. Yao, A. Mar, Y. Wu, $AHgSnQ_4$(A = Sr, Ba; Q = S, Se): A Series of Hg-Based Infrared Nonlinear-Optical Materials with Strong Second-Harmonic-Generation Response and Good Phase Matchability, Inorg. Chem. 58 (2019) 10390-10398.

[5] M. Yan, Z.-D. Sun, W.-D. Yao, W. Zhou, W. Liu, S.-P. Guo, A highly distorted HgS_4 tetrahedron-induced moderate second-harmonic generation response of $EuHgGeS_4$, Inorg. Chem. Front. 7 (2020) 2451-2458.

[6] W. Xing, C. Tang, N. Wang, C. Li, Z. Li, J. Wu, Z. Lin, J. Yao, W. Yin, B. Kang, $EuHgGeSe_4$ and $EuHgSnS_4$: Two Quaternary Eu-Based Infrared Nonlinear Optical Materials with Strong Second-Harmonic-Generation Responses, Inorg. Chem. 59 (2020) 18452-18460.

[7] J. Tang, F. Liang, C. Tang, W. Xing, J. Wu, W. Yin, B. Kang, J. Deng, $SrAgAsS_4$: A Noncentrosymmetric Sulfide with Good Infrared Nonlinear Optical Performance Induced by Aliovalent Substitution from Centrosymmetric $SrGa_2S_4$, Inorg. Chem. 61 (2022) 9205-9212.